DOI: 10.1002/chem.200501070

Rapid and Effective Adsorption of Lead Ions on Fine Poly(phenylenediamine) Microparticles

Mei-Rong Huang, Qian-Yun Peng, and Xin-Gui Li*[a]

Abstract: Fine microparticles of poly(*p*-phenylenediamine) (P*p*PD) and poly(*m*-phenylenediamine) (P*m*PD) were directly synthesized by a facile oxidative precipitation polymerization and their strong ability to adsorb lead ions from aqueous solution was examined. It was found that the degree of adsorption of the lead ions depends on the pH, concentration, and temperature of the lead ion solution, as well as the contact time and microparticle dose. The adsorption data fit the Langmuir isotherm and the process obeyed pseudo-second-order kinetics. According to the Langmuir equation, the maximum adsorption capacities of lead ions onto P*p*PD and P*m*PD microparticles at 30 °C are 253.2 and 242.7 $mg\,g^{-1}$, respectively. The highest adsorptivity of lead ions is up to 99.8 %. The adsorption is very rapid with a loading half-time of only 2 min as well as initial adsorption rates of 95.24 and 83.06 $mg\,g^{-1}\,min^{-1}$ on P*p*PD and P*m*PD particles, respectively. A series of batch experiment results showed that the P*p*PD microparticles possess an even stronger capability to adsorb lead ions than the P*m*PD microparticles, but the P*m*PD microparticles, with a more-quinoid-like structure, show a stronger dependence of lead-ion adsorption on the pH and temperature of the lead-ion solution. A possible adsorption mechanism through complexation between Pb^{2+} ions and =N– groups on the macromolecular chains has been proposed. The powerful lead-ion adsorption on the microparticles makes them promising adsorbents for wastewater cleanup.

Keywords: adsorption · conducting materials · ladder polymers · lead · surface chemistry

Introduction

Heavy-metal ions are among the most feared contaminants in water sources that are beginning to pose severe public health problems nowadays.[1–3] It is well known that heavy-metal ions released into the environment affect ecological life because they tend to accumulate in living organisms and exhibit a high toxicity when adsorbed into the body.[4,5] The removal of heavy-metal ions has been traditionally carried out by several techniques such as membrane processes (for example, dialysis, electrodialysis, reverse-osmosis), neutralization–precipitation and ion exchange, but usually with limited success. In recent years, adsorption has been shown to be an effective and economically feasible alternative method for removal of heavy-metal ions.[6–8] Nonspecific sorbents such as activated carbon,[9,10] metal oxides,[11,12] silica,[13–15] ion-exchange resins, and biosorbents[16] have been used. Specific sorbents have been proposed, consisting of a ligand that can specifically interact with the metal ions, and a carrier matrix that may be an inorganic material (e.g., silica)[14,15,17] or polymers (such as poly(styrene), poly(methacrylate), or poly(vinylbutyral)).[18–22] Polymers have attracted the most attention as carrier matrices because they are easily and effectively produced in a wide variety of compositions, and can be modified into specific sorbents with various functional groups by introducing a variety of ligands[18,21–23] that can greatly improve their ability to remove heavy-metal ions from aqueous solutions.

The search for an effective and economical method of eliminating toxic heavy-metal ions requires the consideration of unconventional materials and processes. Poly(1,8-diaminonaphthalene) microparticles are considered as an efficient sorbent for removal and recovery of Ag^+ ions from aqueous solution,[24–25] exhibiting the highest adsorptivity of Ag^+ ions of 1924 $mg\,g^{-1}$. It has been found that two different reactions occur during the adsorption of Ag^+ ions onto the microparticles, namely complexation adsorption between Ag^+ ions and amine/imine units and the redox ad-

[a] Prof. M.-R. Huang, Q.-Y. Peng, Prof. Dr. X.-G. Li
Institute of Materials Chemistry
College of Materials Science and Engineering
Tongji University, 1239 Siping Road, Shanghai 200092 (China)
Fax: (+86) 21-6598-0524
E-mail: adamxgli@yahoo.com

sorption between Ag^+ ions and free $-NH_2$ groups in the polymer chain. However, the ability of Pb^{2+} ions to adsorb onto the poly(1,8-diaminonaphthalene) microparticles is much weaker, as confirmed in our laboratory. In addition, the 1,8-diaminonaphthalene monomer is relatively expensive.

In this work, we attempt to explore the adsorption behavior of Pb^{2+} ions on microparticles of poly(*p*-phenylenediamine) (P*p*PD)[25,26] and poly(*m*-phenylenediamine) (P*m*PD).[25,27] The *p*-phenylenediamine and *m*-phenylenediamine compounds are important and also cheap derivatives of aniline, and exhibit a high oxidative polymerization yield.[25–28] Many =N− groups on the P*p*PD and P*m*PD chains may efficiently bind Pb^{2+} ions.[25–27] For this purpose, the fine, nontoxic, and odor-free microparticles were prepared by a simple oxidative precipitation polymerization from *p*- and *m*-phenylenediamines and their structure was characterized by IR spectroscopy, wide-angle X-ray diffraction analysis, and laser particle-size analysis. In particular, various important factors affecting the Pb^{2+} adsorption onto the microparticles, such as pH, concentration, and temperature of Pb^{2+} solution, as well as adsorption time, the structure and dosage of the microparticles, were systematically investigated by using batch experiments. To the best of our knowledge, this work represents the first example of Pb^{2+} ion adsorption onto poly(phenylenediamine) microparticles.

Results and Discussion

Synthesis of poly(phenylenediamine) microparticles: The chemical oxidative polymerization of three phenylenediamine isomers in 1 M HCl, water, and glacial acetic acid simply afforded uniform and fine polymer microparticles as products (Scheme 1). As listed in Table 1, the polymerization yield strongly depends on the monomer structure and also the polymerization medium. The yield of P*m*PD is much higher in water than in HCl, while the yield of P*p*PD and poly(*o*-phenylenediamine) (P*o*PD) is higher in HCl and glacial acetic acid (GA) respectively, because the P*p*PD and P*o*PD microparticles that polymerized in water as the polymerization medium are partially water-soluble. The lower polymerization yield of the *p*- and *o*-phenylenediamines in water and *m*-phenylenediamine in HCl should be attributable to their lower molecular weight that results from a weaker ability to polymerize in the corresponding medium. This suggests that the oxidative polymerization mechanism changes significantly with monomer structure[25–28] and polymerization medium, leading to a different macromolecular structure, as illustrated in Scheme 1 and discussed below.

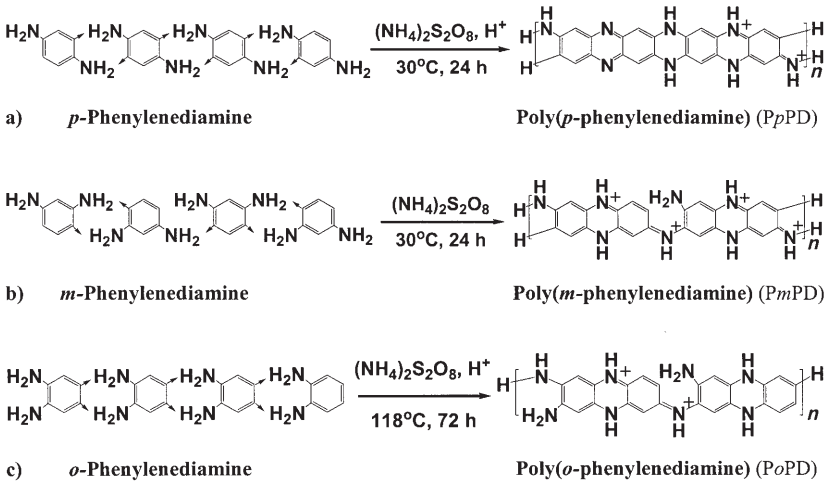

Scheme 1. Chemical oxidation polymerization of *p*-, *m*-, and *o*-phenylenediamines.[25]

Table 1. Preparation and properties of salt microparticles of three poly(phenylenediamine)s by a chemically oxidative precipitation polymerization reaction with phenylenediamine/oxidant molar ratio of 1:1 for a polymerization time of 24 h.

Polymer microparticles	Polymerization medium	temp [°C]	yield [%]	color	Properties of the as-prepared polymer salt microparticles: solubility in H_2O, 10 mM HCl, and NaOH	electrical conductivity [S cm^{-1}]	Pb^{2+} adsorption[a]: capacity [mg g^{-1}]/ adsorptivity [%]	Pb^{2+} adsorption[a]: maximal capacity [mg g^{-1}] Q_{max} [mg g^{-1}]	Ag^+ adsorption[c]: capacity[b]/adsorptivity [%]
P*p*PD(HCl)	1 M HCl	30	90	black	insoluble	3.2×10^{-5}	182/73	253.2	373/6.8
P*p*PD(H_2O)	H_2O	30	80	black	partly soluble	2.6×10^{-5}	[d]		
P*m*PD(HCl)	1 M HCl	30	45	black	insoluble	1.2×10^{-3}	81/32	126.4	684/12.8
P*m*PD(H_2O)	H_2O	30	83	black	insoluble	1.5×10^{-3}	177/71	242.7	200/4.6
P*o*PD(GA)[e]	glacial CH_3COOH	118	96	black	insoluble	low	150/60	195.5	540/1.2
P*o*PD(H_2O)	H_2O	100	80	dark red	partly soluble	very low	[d]		

[a] The adsorption of Pb^{2+} onto poly(phenylenediamine) microparticles at 30 °C and pH 4.9 in $Pb(NO_3)_2$ solution (25 mL) at an initial Pb^{2+} concentration of 500 mg L^{-1} with 50 mg of sorbent for 24 h. [b] Maximum capacity Q_{max} simulated by the Langmuir isotherm. [c] The adsorption of Ag^+ ions onto poly(phenylenediamine) microparticles at 30 °C and pH 5.3 in $AgNO_3$ solution (25 mL) at an initial Ag^+ concentration of 110 mM with 50 mg of sorbent for 24 h. [d] Not measured because partially water-soluble polymers could not be used as adsorbents. [e] The polymerization time is 72 h.

Structure of poly(phenylenediamine) microparticles: We studied the microparticle macromolecular structures of P*p*PD with HCl as the polymerization medium (P*p*PD-(HCl)) and P*m*PD with water as the polymerization medium (P*m*PD(H_2O)) by IR spectroscopy (Figure 1).

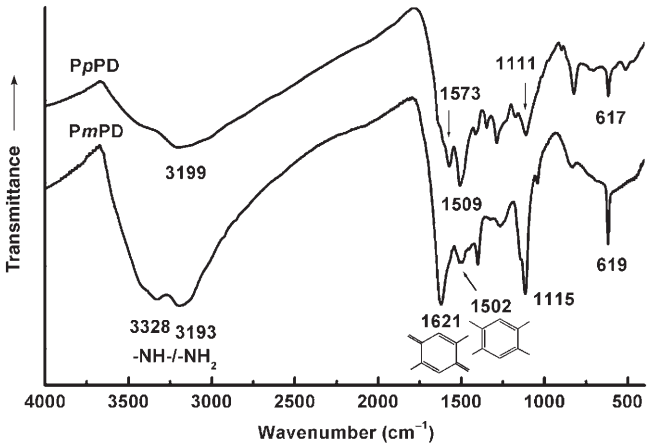

Figure 1. IR spectra of poly(*p*-phenylenediamine) salt microparticles (PpPD(HCl)) with HCl as polymerization medium and poly(*m*-phenylenediamine) salt microparticles (PmPD(H_2O)) with water as polymerization medium.

Broad and strong bands at 3193 and 3328 cm^{-1}, due to the characteristic stretching vibration of N–H, suggest the presence of a large number of imino and amino groups (–NH–/$-NH_2$) in the spectra of both polymers. In particular, the spectrum of P*m*PD exhibits much stronger bands at 3199 and 3328 cm^{-1} than P*p*PD, implying that there are many more –NH–/$-NH_2$ groups in the P*m*PD chains. In addition, both polymers exhibit different characteristic spectral bands in the wavenumber range 450–2000 cm^{-1}. The spectrum of P*p*PD shows a more intense band around 1509 cm^{-1} than that around 1573 cm^{-1}. On the contrary, the P*m*PD spectrum shows a less-intense band around 1502 cm^{-1} than that around 1621 cm^{-1}. The P*m*PD spectrum also displays much more intense bands at 1115 and 619 cm^{-1}, which are attributed to the in-plane and out-of-plane bending vibration of the C–H bonds of 1,2,4-trisubstituted benzene rings, respectively. These facts prove that the molecular structure of P*p*PD is different from that of P*m*PD (Scheme 1).[26,27,29]

The supramolecular structures of P*p*PD(HCl) and P*m*PD-(H_2O) microparticles have been characterized by wide-angle X-ray diffraction studies (Figure 2), which show different amorphous structure characteristics that are coincident with the molecular structure. The spectrum of P*p*PD shows a broad diffraction peak centered at the Bragg angle of 25°, together with several sharp peaks at 20.4°, 22.7°, and 29.2° that are ascribed to a very small amount of residual inorganic salt (the reductive product of the oxidant $(NH_4)_2S_2O_8$: $(NH_4)_2SO_4$) trapped inside the particles, because the spectrum of the doped particles (salt) obtained after soaking and washing with water does not show any sharp diffraction peaks (Figure 2c). The spectrum of the undoped particles

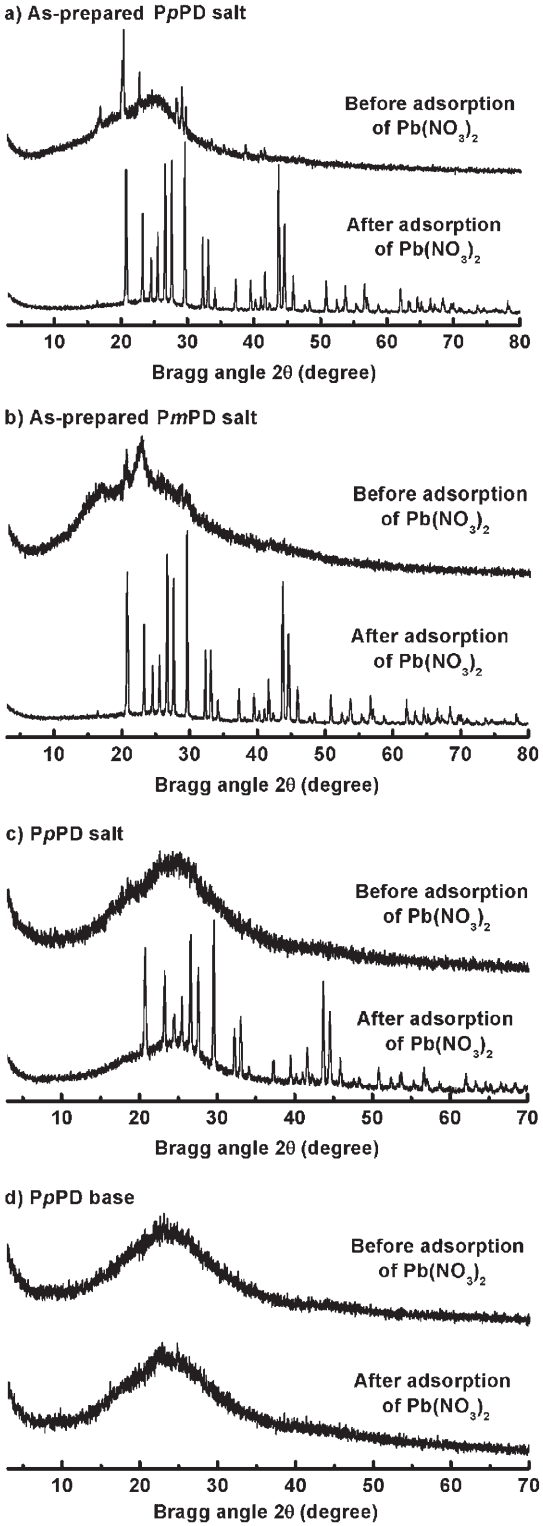

Figure 2. Wide-angle X-ray diffractograms of: a) as-prepared P*p*PD salt microparticles; and b) as-prepared P*m*PD salt microparticles before and after adsorption of Pb^{2+} ions in $Pb(NO_3)_2$ aqueous solution (25 mL), at an initial Pb^{2+} concentration of 800 mg L^{-1} at 30 °C, with 50 mg of adsorbent for 24 h; as well as c) P*p*PD salt after soaking in water; and d) P*p*PD base before and after adsorption for Pb^{2+} ions under the same adsorption conditions as above but in 200 mg L^{-1} $Pb(NO_3)_2$ aqueous solution.

(base) procured after a treatment with NH_4OH also does not exhibit any sharp diffraction peaks (Figure 2d). The spectrum of P*m*PD has two broad and merged diffraction peaks centered at the Bragg angles of 23° and 17°, together with one sharp peak at 20.4° due to an inorganic impurity. P*p*PD microparticles exhibit slightly lower crystallinity possibly due to the slightly higher aromaticity of the P*p*PD chains compared to that of the P*m*PD chains (Scheme 1). A different molecular structure is likely to be responsible for the different supramolecular structure. An amorphous structure should favor the penetration into and then adsorption of lead ions onto the microparticles because the macromolecular chains in the amorphous structure are piled in a more loose and disordered way than those in the crystalline structure.

The adsorption and adsorption mechanism of Pb^{2+} ions onto poly(phenylenediamine) microparticles: As summarized in Table 1, the properties of the microparticles are strongly influenced by the monomer species. We note that only P*p*PD(HCl) and P*m*PD(H_2O) fine microparticles with high polymerization yield, high bulk electrical conductivity, and good insolubility in water, HCl, and NaOH aqueous solutions, exhibit a strong capability for Pb^{2+} ion adsorption. In addition, P*m*PD(HCl) and P*o*PD(GA) microparticles exhibit a lower Pb^{2+} ion adsorption and a greater capability to adsorb Ag^+ ions but the ability to adsorb the Ag^+ ions is still much lower than that onto poly(1,8-diaminonaphthalene) microparticles.[24] This could be due to the presence of many more $-NH_2$ groups in the poly(1,8-diaminonaphthalene) chains than in the P*p*PD(HCl) and P*m*PD(H_2O) chains. Therefore, the adsorption mechanism of Pb^{2+} and Ag^+ ions onto the polymer particles is quite different in that there is a complexation adsorption of Pb^{2+} ions but a redox adsorption of Ag^+ ions. Note that microparticles of poly(*o*-phenylenediamine) with glacial acetic acid as polymerization medium (P*o*PD(GA)) could be successfully prepared only at 118 °C over a long time. Consequently, it seems that the P*p*PD(HCl) and P*m*PD(H_2O) microparticles could be suitable for Pb^{2+} adsorption due to the combination of high Pb^{2+} adsorptivity, low preparation cost, and good insolubility in water, acidic, and alkaline solution.

We further confirmed the occurrence of Pb^{2+} adsorption onto the P*p*PD and P*m*PD microparticles by observing the variation of the wide-angle X-ray diffraction spectra and conductivity of the microparticles with Pb^{2+} adsorption. The spectra of the three P*p*PD and P*m*PD salts absorbing Pb^{2+} ions display a series of new sharp X-ray diffraction peaks (Figure 2a–c) as compared with the original polymer salts, but the P*p*PD base absorbing Pb^{2+} does not exhibit any sharp peaks in the spectra shown in Figure 2d. The characteristics of the sharp peaks indicate the presence of $PbSO_4$ from a reaction between Pb^{2+} ions and a SO_4^{2-} group rather than $Pb(NO_3)_2$. The SO_4^{2-} group could result from residual free sulfate and doping sulfuric acid in the particles because the soaked salt particles adsorbing Pb^{2+} ions exhibit weaker diffraction peaks (Figure 2c), whereas the base particles adsorbing 30 mg Pb^{2+} per gram of the particles do not exhibit any peak indicative of a crystalline structure in their spectrum (Figure 2d). This signifies that the Pb^{2+} ion adsorption on the base particles results from the complexation between Pb^{2+} ions and macromolecular chains. However, the complexation and precipitation adsorptions of lead ions onto the salt particles occur simultaneously. Additionally, the conductivity of the Pb^{2+}-adsorbing salt particles is around four times higher than that compared with Pb^{2+}-free particles. These results indicate a real uptake of Pb^{2+} ions onto the P*p*PD and P*m*PD particles. On the basis of these results and the data listed in Table 1, the as-prepared P*p*PD(HCl) and P*m*PD(H_2O) salt microparticles have been chosen as cost-effective Pb^{2+} adsorbents in the following study on the effect of several important factors on Pb^{2+} ion adsorption.

Generally, the main adsorption sites for lead ions are at the $=N-$ groups in the macromolecular chains because the nitrogen atom has a lone pair of electrons that can efficiently bind a metal ion through sharing an electron pair to form a metal complex. Considering this, a possible adsorption mechanism by complexation between Pb^{2+} ions and $=N-$ groups on the polymer chains of the P*p*PD(HCl) and P*m*PD(H_2O) particles is proposed in Figure 3.

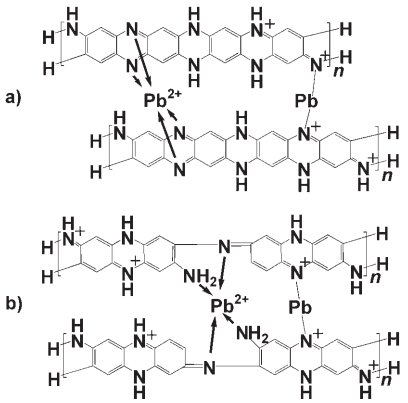

Figure 3. Possible complexation and ion exchange between lead ions and $=N-/=N^+H-$ groups on the macromolecular chains of the P*p*PD(HCl) (a) and (P*m*PD(H_2O)) (b) salt microparticles.

It is known that there should be some $=N^+H-$ groups in the chain structure of the microparticles obtained in acidic and neutral aqueous solution. Therefore, another possible route for the Pb^{2+} ion adsorption is ion exchange between Pb^{2+} and the H^+ ions on the $=N^+H-$ group. This has been confirmed by the fact that the final pH value of the resultant $Pb(NO_3)_2$ solution after adsorption was invariably lower than the initial pH value (Table 2). Note that after the blank water was treated by the microparticles, we observed a slight decrease in the solution pH value. This could also be attributable to the release of H^+ ions due to the exchange of $=N^+H-$ groups on the chain structure of the microparticles by trace amounts of the metal ions in the water. The pH decrease of the blank water after a treatment of the mi-

Table 2. The change of the solution pH after Pb^{2+} ion adsorption at 30 °C in 25 mL solution with 50 mg of adsorbent (as-prepared P*p*PD and P*m*PD salt particles) for 24 h.

Adsorbent	Pb^{2+} ion concentration in the solution [mg L^{-1}]								
	0 (blank water)			500			800		
	before	after	ΔpH	before	after	ΔpH	before	after	ΔpH
P*p*PD	6.5	6.3	−0.2	4.9	3.0	−1.9	4.8	2.9	−1.9
P*m*PD	6.5	6.1	−0.4	4.9	2.9	−2.0	4.8	3.0	−1.8

croparticles indicates that some H^+ ions are released into the solution as the Pb^{2+} ions are bound on the particles. Consequently, the Pb^{2+} adsorption may also occur by an ion exchange between Pb^{2+} and H^+ ions on the microparticles.

It should be noted that an exchange reaction between Pb^{2+} and $=N^+H-$ could be slower than the complexation reaction between Pb^{2+} ions and $=N-$ due to stronger electrostatic repulsion between the Pb^{2+} ions and $=N^+H-$ as opposed to the $=N-$ groups. At the same time, there are relatively more $=N^+H-/=N-$ groups. Thus, we could speculate that the complexation may be dominant during Pb^{2+} ion adsorption. On the basis of the above discussion, the pH value of the Pb^{2+} solution is one of the factors influencing Pb^{2+} ion adsorption performance on the microparticles, as discussed below.

Effect of solution pH on the Pb^{2+} ion adsorption: To examine the effect of solution pH on Pb^{2+} ion adsorption onto the microparticles, the initial pH of the $Pb(NO_3)_2$ aqueous solution was adjusted to between 1.0–7.0 by adding a certain amount of 0.05 M HNO_3 or NaOH. If the pH value is higher than 7.0, then precipitation of $Pb(OH)_2$ in the basic medium is expected. Figure 4 shows the variation of Pb^{2+} ion adsorption with the pH value of Pb^{2+} solution at an initial Pb^{2+} ion concentration of 200 mg L^{-1} at 30 °C. We observed that the adsorption capacity and adsorptivity of Pb^{2+} ions onto the poly(phenylenediamine) microparticles both increased significantly in the pH range 2.5–4.2 but increased only slightly in the pH range 4.2–7.0, the highest values being at pH 7.0. This behavior could be ascribed to a competitive adsorption of Pb^{2+} over H^+ ions to the nitrogen atom on the surface of the poly(phenylenediamine) particles.[9] The protonation of the adsorption sites is dominant at low pH. With increasing initial pH values of Pb^{2+} solution, the number of protonated $=N^+H-$ groups would decrease and thus the amount of neutral $=N-$ groups present on the particle surface would increase, resulting in an increase in Pb^{2+} ion adsorption. This could explain the fact that the P*m*PD microparticles containing more $=N-$ groups (Figure 3) always demonstrate stronger sensitivity of Pb^{2+} ion adsorption to pH value in a pH range from 2.5 to 5.0 than the P*p*PD microparticles. In addition, the binding of a Pb^{2+} ion to a nitrogen atom could be stronger than that of an H^+ ion since the electrical attraction force between the lone pair of electrons from the nitrogen atom and the divalent Pb^{2+} ion would be stronger than that between the lone pair of electrons and the monovalent proton (H^+). By the way, a small variation of the adsorption capability in the pH range between 4.2 and 7.0 facilitates the practical application to some extent. It should be noticed that P*p*PD microparticles always exhibit stronger Pb^{2+} ion adsorption than P*m*PD particles under the same conditions. The highest adsorption capacity and adsorptivity of lead ions on P*p*PD microparticles at pH 7.0 are found to be 89.8 mg g^{-1} and 86.9 %, respectively.

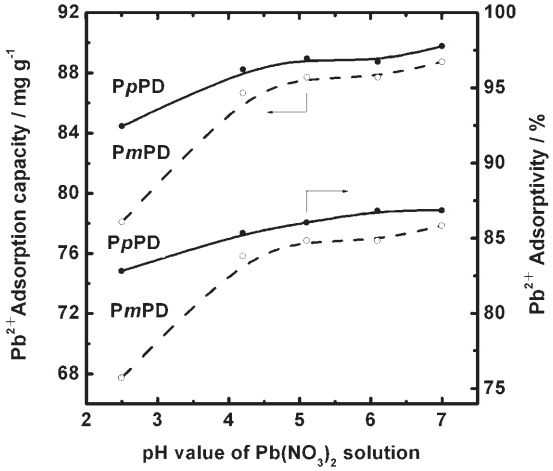

Figure 4. Effect of pH value on adsorption of Pb^{2+} ions onto as-prepared P*p*PD and P*m*PD salt particles at 30 °C in $Pb(NO_3)_2$ solution (25 mL) at the initial Pb^{2+} concentration of 200 mg L^{-1} with 50 mg of adsorbent for 24 h.

On the other hand, the Pb^{2+} ion adsorption is also influenced by the transport of lead ions from the bulk solution to the $=N^+H-$ sites on the particle surface. The transport of Pb^{2+} could be prevented at low pH because the strong electrostatic repulsion from a large number of protonated $=N^+H-$ groups would prevent Pb^{2+} ions from approaching close enough to the particle surface. The increase of Pb^{2+} ion adsorption with increasing pH is apparently attributable to the weak electrostatic repulsion due to weak protonation at the high pH value. This could also explain the weak Pb^{2+} ion adsorption at low pH in Figure 4.

Effect of solution temperature on the Pb^{2+} ion adsorption: We studied the effect of $Pb(NO_3)_2$ solution temperature on the Pb^{2+} adsorption in a temperature range of 10–50 °C. As shown in Figure 5, the adsorption of Pb^{2+} ions on the P*p*PD and P*m*PD microparticles increases steadily with increasing temperature. Particularly, the P*m*PD microparticles exhibit a faster increase of the adsorption with temperature rise than the P*p*PD microparticles, implying that the molecular and supramolecular structures of P*m*PD microparticles with more quinoid-like and $=N^+H-$-group-containing structures (Figures 1 and 3) are more sensitive to temperature, since the interchain interaction from positively charged $=N^+H-$ groups readily changes with temperature.

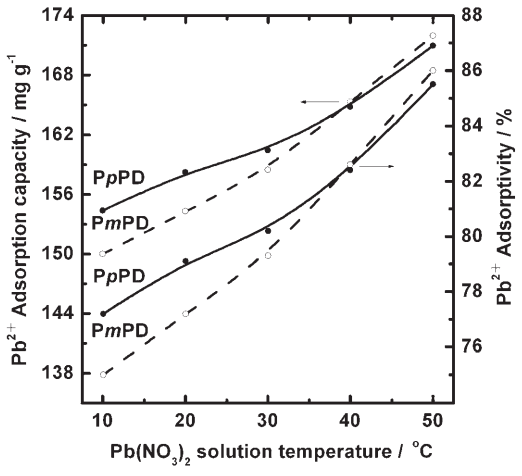

Figure 5. Effect of temperature on the adsorption of Pb^{2+} on as-prepared P*p*PD and P*m*PD salt particles in $Pb(NO_3)_2$ solution (25 mL) at an initial Pb^{2+} concentration of 400 mg L^{-1} with 50 mg of adsorbent at pH 5.0 for 24 h.

Therefore, the P*m*PD microparticles demonstrate the highest adsorption capacity up to 172 mg g^{-1} and the highest adsorptivity of up to 86.0% at 50°C. The fact that high temperature favors the Pb^{2+} ion adsorption could be explained by the higher activity of the reactive sites at higher temperature.

The effect of Pb^{2+} solution temperature on sorption is further corroborated by the van't Hoff plot based on Equation (1),[7] where the equilibrium constant K_d is defined as Q_e/C_e, Q_e [mg g^{-1}] is the amount of Pb^{2+} ions adsorbed onto the P*p*PD and P*m*PD particles at equilibrium concentration C_e [mg L^{-1}], T [K] the absolute temperature, R the gas constant (8.314 J mol^{-1} K^{-1}), $\Delta S^\ominus$ the entropy change [J mol^{-1}], and $\Delta H^\ominus$ is the enthalpy change [kJ mol^{-1}].

$$\log K_d = (\Delta S^\ominus/2.303\,R) - (\Delta H^\ominus/2.303\,RT) \quad (1)$$

The plots of log K_d versus $1/T$ for the adsorption process are found to be linear. $\Delta H^\ominus$ and $\Delta S^\ominus$ calculated from the slope and intercept of the plots are 9.90 kJ mol^{-1} and 39.05 J mol^{-1} for P*p*PD, and 13.34 kJ mol^{-1} and 50.01 J mol^{-1} for P*m*PD, respectively. The positive $\Delta H^\ominus$ indicates the endothermic nature of the adsorption. The relatively small $\Delta S^\ominus$ values imply a slightly increased randomness at the solid–solution interface during adsorption, and no significant structural change occurs inside the adsorbents. Similar positive $\Delta H^\ominus$ values have been reported by Manju and co-workers with the adsorption of Pb^{2+} ions from wastewater by poly(acrylamide)-grafted iron(III) oxide.[7]

Further, we can evaluate the Gibbs free energy change ($\Delta G^\ominus$) by using Equation (2).

$$\Delta G^\ominus = \Delta H^\ominus - T\Delta S^\ominus \quad (2)$$

The $\Delta G^\ominus$ values calculated range from −2.82 to −0.82 kJ mol^{-1} for P*m*PD and −2.72 to −1.16 kJ mol^{-1} for P*p*PD, respectively, in the examined temperature range, as shown in Figure 6. The negative $\Delta G^\ominus$ indicates the feasibility of the process and the spontaneous nature of adsorption.

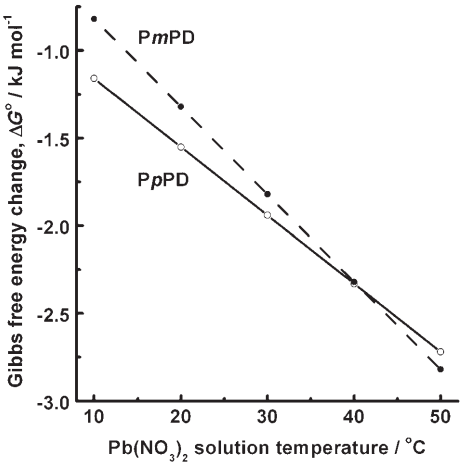

Figure 6. The variation of the $\Delta G^\ominus$ values for the $Pb(NO_3)_2$ solution during the adsorption of Pb^{2+} ions onto the as-prepared P*p*PD(HCl) and P*m*PD(H_2O) salt microparticles with solution temperature.

The $\Delta G^\ominus$ values decrease with increasing temperature, strongly suggesting that the Pb^{2+} ion adsorption becomes more feasible at higher temperatures. Stronger dependency of the $\Delta G^\ominus$ value on the temperature for the P*m*PD than for the P*p*PD can also be attributable to more $=N^+H-$ groups on the P*m*PD particles.

Optimization of poly(phenylenediamine) microparticle dosage: Figure 7 shows the adsorption capacity and adsorptivity of Pb^{2+} ions as a function of P*m*PD microparticle dosage. The adsorption capacity exhibits a maximum at a dosage of 50 mg. Correspondingly, the adsorptivity increases linearly with increasing dosage from 10 to 70 mg and then reaches a plateau at above 97% in a dosage range of 70–100 mg. The highest adsorptivity occurring in this study is 99.8% at the particle dosage of 100 mg. An even higher adsorptivity might be achieved if the particle dosage were higher. In other words, almost all Pb^{2+} ions would be adsorbed onto the microparticles if the particle dosage is higher than 100 mg. In the practical adsorption, however, unilaterally increasing particle dosage leads to a sharp decrease of the adsorption capacity and thus to a waste of sorbent. Therefore, we have to balance adsorption capacity and adsorptivity by choosing an optimal particle dosage. An optimal dosage of P*m*PD microparticles is around 67 mg in this adsorption system.

Optimization of initial Pb^{2+} ion concentration and adsorption isotherm: Adsorption of Pb^{2+} ions onto P*p*PD and P*m*PD microparticles is given as a function of initial Pb^{2+} ion concentration in Figure 8. We found that the two types of microparticles show a similar adsorption behavior to-

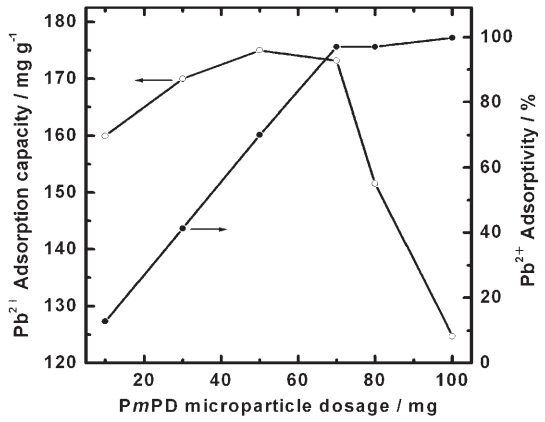

Figure 7. Effect of the dosage of as-prepared P*m*PD(H_2O) salt particles on adsorption of Pb^{2+} ions at 30 °C and pH 5.0 in $Pb(NO_3)_2$ solution (25 mL) at Pb^{2+} ion concentration of 500 mg L^{-1} for 24 h.

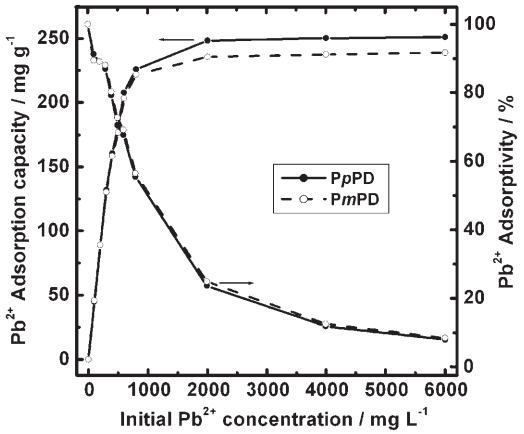

Figure 8. Effect of initial Pb^{2+} concentration on Pb^{2+} adsorption onto as-prepared P*p*PD(HCl) and P*m*PD(H_2O) salt microparticles at 30 °C and pH 5.0 in $Pb(NO_3)_2$ solution (25 mL) with a microparticle dosage of 50 mg for 24 h.

wards Pb^{2+} ions. Just like most other adsorbents,[9] the adsorption capacity rises significantly with an increase in the Pb^{2+} ion concentration in the range of 0–800 mg L^{-1}, while the Pb^{2+} ion adsorptivity declines gradually. Consequently, both the adsorption capacity and adsorptivity of the Pb^{2+} ions simultaneously reach a high level at the optimal initial Pb^{2+} concentration of around 550 mg L^{-1}.

The adsorption isotherm for Pb^{2+} ions onto P*p*PD and P*m*PD microparticles is shown in Figure 9. To establish a quantitative relationship between ion concentration and the adsorption process, two linearized mathematical models proposed by Langmuir and Freundlich were used to describe and analyze the adsorption isotherm and equilibrium, as listed in Equations (3) and (4), where Q_m is the adsorption capacity at saturation

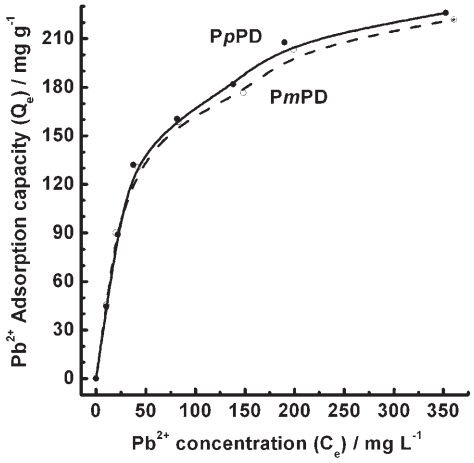

Figure 9. Adsorption isotherms of Pb^{2+} ions on as-prepared P*p*PD and P*m*PD salt microparticles at 30 °C and pH 5.0 in $Pb(NO_3)_2$ solution (25 mL) with microparticle dosage of 50 mg for 24 h.

(mg g^{-1}), K_a the adsorption coefficient (L mg^{-1}), K_F the equilibrium constant indicating adsorption capacity, and n is the adsorption equilibrium constant.

$$C_e/Q_e = C_e/Q_m + 1/(K_a Q_m) \quad (3)$$

$$\log Q_e = (1/n)\mathrm{Log}\, C_e + \mathrm{Log}\, K_F \quad (4)$$

These constants were evaluated from the intercept and the slope, respectively, of the linear plots of C_e/Q_e versus C_e, and $\mathrm{Log}\, Q_e$ versus $\mathrm{Log}\, C_e$, based on experimental data through a regression analysis. The obtained parameters and the correlation coefficients are listed in Table 3. The results show that the adsorption behavior of Pb^{2+} ions onto P*p*PD and P*m*PD microparticles is better described by the Langmuir isotherm than by the Freundlich isotherm because the Langmuir model yields a higher correlation coefficient and lower standard deviation.[14]

Adsorption kinetics of Pb^{2+} ions onto poly(phenylenediamine) microparticles: The time-course experiments were carried out by stirring the adsorption mixture at various predetermined intervals and analyzing the Pb^{2+} ion content after a certain contact time. The adsorption kinetics were studied to determine the time required to reach the equilibrium adsorption of Pb^{2+} ions. Figure 10 shows a representative plot of the Pb^{2+} ion adsorption capacity and adsorptivity versus adsorption time for the P*p*PD(HCl) microparticles. Apparently, the adsorption rate of Pb^{2+} ions onto the

Table 3. Isotherm model equations for Pb^{2+} ion adsorption onto as-prepared P*p*PD and P*m*PD salt microparticles based on the data presented in Figure 9.

Mathematical model	Sorbent	Equation	Correlation coefficient	Standard deviation	Q_m [mg g^{-1}]	K_a [L mg^{-1}]
Langmuir	P*p*PD	$C_e/Q_e = 0.00395C_e + 0.1745$	0.9986	0.0282	253.2	0.0225
	P*m*PD	$C_e/Q_e = 0.00412C_e + 0.1651$	0.9982	0.0346	242.7	0.0250
Freundlich	P*p*PD	$\log Q_e = 0.4336 \log C_e + 1.3286$	0.9482	0.0864		
	P*m*PD	$\log Q_e = 0.4031 \log C_e + 1.3809$	0.9627	0.0715		

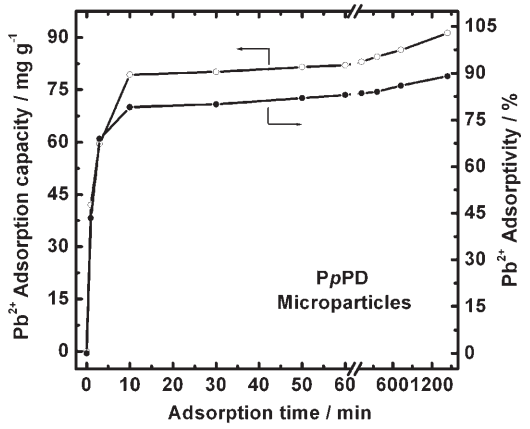

Figure 10. Effect of adsorption time on the ability of Pb^{2+} ions to adsorb onto as-prepared P*p*PD at 30 °C and pH 5.0 in $Pb(NO_3)_2$ solution (25 mL) at an initial Pb^{2+} ion concentration of 200 mg L^{-1} with 50 mg adsorbent.

microparticles is very rapid during the initial 10 min but becomes slow during the adsorption time from 10 to 1500 min. The adsorption capacity and adsorptivity at the adsorption time of 10 min are 80 mg g^{-1} and 80 % respectively.

The adsorption of Pb^{2+} ions on the microparticles increases nonlinearly with increasing adsorption time. The adsorption process can be divided into two steps: a primary rapid step and a secondary slow step. The rapid step lasts for about 10 min and the loading half-time is found to be only 2 min. The fast step of Pb^{2+} ion adsorption may occur on the microparticle surfaces due to an immediate interaction between Pb^{2+} ions and the active $=N-/=N^+H-$ groups in the polymer chains, while the slow step may occur inside the microparticles, representing the diffusion of Pb^{2+} ions into the interior of the microparticles over the period.

To gain some insight into the adsorption kinetics of the removal of Pb^{2+} ions by the microparticles, we used the experimental data in the pseudo-first-order and pseudo-second-order kinetics equations. The adsorption-rate expressions are given in Equations (5) and (6),[30,31] where Q_e is the equilibrium amount of Pb^{2+} ions adsorbed (mg g^{-1}), Q_t the amount adsorbed (mg g^{-1}) at a certain time t, k' the rate constant of pseudo-first-order adsorption (min^{-1}), and h the initial adsorption rate of pseudo-second-order adsorption (mg g^{-1} min^{-1}).

$$\log(Q_e - Q_t) = \log Q_e - k't/2.303 \text{ (pseudo-first-order)} \quad (5)$$

$$t/Q_t = t/Q_e + 1/h \text{ (pseudo-second-order)} \quad (6)$$

The curves of $\log(Q_e - Q_t)$ versus t and t/Q_t versus t based on the data during the contact time from zero to 60 min in Figure 10 (the data for P*m*PD were omitted) provide the corresponding parameters, as listed in Table 4. We see that an application of the pseudo-second-order model correlates better with the experimental data than the pseudo-first-order model.[7] Thus the system under study is more appropriately described by a pseudo-second-order kinetics model that is based on the assumption that the rate-limiting step may be chemical sorption involving valency forces through sharing or exchange of electrons between sorbent and sorbate. The initial adsorption rates of Pb^{2+} ions onto P*p*PD and P*m*PD microparticles are 88.03 and 81.83 mg g^{-1} min^{-1} respectively, and are much higher than the h value found with rice huck when used for the adsorption of Pb^{2+} ions.[32]

A comparison of Pb^{2+} adsorption onto the microparticles and other sorbents: As discussed above, the highest Pb^{2+} adsorption capacities are found to be 253.2 and 242.7 mg g^{-1} for P*p*PD(HCl) and P*m*PD(H_2O) respectively. Although a direct comparison of performance of P*p*PD and P*m*PD with other adsorption materials is difficult owing to different adsorption conditions, it is important that the highest Pb^{2+} adsorption capacities of both P*p*PD and P*m*PD are even higher than those of nanoporous activated carbon (121.2 mg g^{-1})[33] and other better absorbents, such as hydrated iron(III)-oxide-grafted poly(acrylamide) (211.4 mg g^{-1}),[7] modified microporous poly(2-hydroxyethyl methacrylate) (174.2 mg g^{-1}),[21] dithizone-anchored poly(2-hydroxyethyl methacrylate) microbeads (155.2 mg g^{-1}),[22] and modified poly(vinylbutyral) microbeads (86.2 mg g^{-1}).[19] In fact, the Pb^{2+} ion adsorption capacity on P*p*PD is close to that of microporous titanosilicate (231.8 mg g^{-1})[13] and hybrid macroporous modified silica (256.7 mg g^{-1}).[14]

The adsorption rate of Pb^{2+} ions onto P*p*PD and P*m*PD microparticles is much faster than that onto oxidized nanoporous activated carbon,[33] iron(III)-oxide-grafted poly(acrylamide),[7] and poly(vinylbutyral) microbeads.[19] It is reported that the respective equilibrium adsorption time of Pb^{2+} ions onto the activated carbon and poly(acrylamide) is about 24 and 4 h, respectively, and that onto poly(vinylbutyral) for 50 % adsorption is 7 min, whereas the adsorption time of Pb^{2+} ions onto the P*p*PD and P*m*PD microparticles for 50 % adsorption is around 2 min. Similarly, the P*p*PD and P*m*PD microparticles also exhibit higher Pb^{2+} ion adsorption capacity than some natural materials, as shown in Figure 11, especially at the initial Pb^{2+} concentration with sorbent amounts of 200–4000 mg g^{-1}. It should be noted that

Table 4. Kinetics model equations for Pb^{2+} ion adsorption on as-prepared P*p*PD and P*m*PD salt microparticles.

Mathematical model	Sorbent	Equation	Correlation coefficient	Standard deviation	Rate constant (k) [min^{-1}] or initial adsorption rate (h) [mg g^{-1} min^{-1}].
pseudo-first-order	P*p*PD	$\log(Q_e - Q_t) = -0.01273t + 1.96$	−0.7964	0.2637	$k = 0.0293$
	P*m*PD	$\log(Q_e - Q_t) = -0.01450t + 1.94$	−0.6704	0.4259	$k = 0.0334$
pseudo-second-order	P*p*PD	$t/Q_t = 0.01203t + 0.01136$	0.99995	0.00344	$h = 88.03$
	P*m*PD	$t/Q_t = 0.01192t + 0.01222$	0.999	0.00574	$h = 81.83$

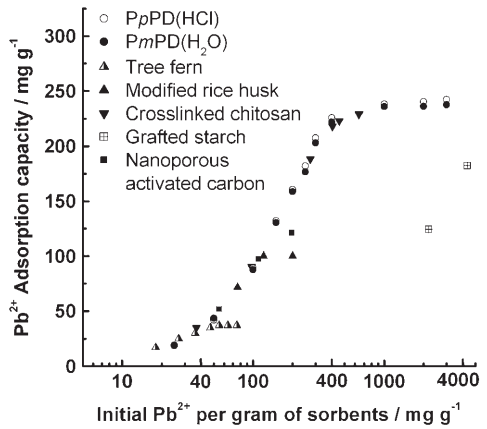

Figure 11. A comparison of adsorption capacity for Pb^{2+} ions onto as-prepared P*p*PD and P*m*PD salt particles and other efficient sorbents.

all of these synthetic absorbents are obtained by relatively complicated preparation procedures (low productivity and high cost). However, the preparation of the P*p*PD(HCl) and P*m*PD(H_2O) microparticles through a chemical oxidative precipitation polymerization is very simple and highly efficient, producing nontoxic and odourless microparticles, and demonstrating an important potential application as a highly efficient Pb^{2+} sorbent.

Conclusion

Fine P*p*PD and P*m*PD microparticles have been successfully synthesized by a facile oxidative precipitation polymerization procedure. The adsorption of Pb^{2+} ions onto the microparticles has been optimized by regulating the pH and concentration of the Pb^{2+} solution, as well as the adsorption time and microparticle dosage. The adsorption data fitted the Langmuir isotherm and followed pseudo-second-order reaction kinetics. The thermodynamic parameters confirmed the feasibility and spontaneous nature of the Pb^{2+} ion adsorption process on the microparticles. The adsorption consists of two steps, the first being fast reaction adsorption on the particle surface and the second being slow interior adsorption inside the particles. The maximum adsorption capacities of Pb^{2+} ions onto the P*p*PD and P*m*PD microparticles are 253.2 and 242.7 $mg\,g^{-1}$, respectively. The highest achievable Pb^{2+} ion adsorptivity is 99.8%. The Pb^{2+} ion adsorption onto the P*p*PD and P*m*PD microparticles is very rapid with initial adsorption rates of 95.24 and 83.06 $mg\,g^{-1}\,min^{-1}$, respectively. The P*p*PD microparticles demonstrate higher Pb^{2+} adsorption than the P*m*PD microparticles, but the P*m*PD microparticles with more $=N^{+}H-$ groups illustrate a stronger dependence of Pb^{2+} ion adsorption on the pH and temperature of the Pb^{2+} solution. That is to say, the Pb^{2+} ion adsorption behavior onto the microparticles significantly depends on their molecular structure. The rapid uptake and greater adsorption of Pb^{2+} ions, along with simple preparation of the microparticles and low cost of the raw materials, make them very attractive and cost-effective as highly efficient sorbents for the removal of Pb^{2+} ions from aqueous solutions.

Experimental Section

Chemical reagents: *p*-Phenylenediamine (*p*PD), *m*-phenylenediamine (*m*PD), *o*-phenylenediamine (*o*PD), ammonium persulfate and lead nitrate of Analytical Reagent grade were obtained commercially and used as received.

Preparation of the fine microparticles as adsorbents: Two batches of fine polymer microparticles from *p*-phenylenediamine and *m*-phenylenediamine were synthesized by chemical oxidative polymerization reactions in HCl aqueous solution (1 M) or distilled water by using ammonium persulfate as an oxidant.[29,34,35] A typical procedure for preparation of poly(*p*-phenylenediamine), P*p*PD, was as follows: *p*-phenylenediamine (2.163 g, 20 mmol) and ammonium persulfate (4.564 g, 20 mmol) were dissolved in HCl aqueous solution (1 M, 50 mL), respectively, to prepare a monomer solution and an oxidant solution. The monomer solution was then stirred and treated with the oxidant solution dropwise at a rate of one drop (60 μL) every 3 s over 30 min at 30 °C. Immediately after the addition of the first drop, the solution turned blue-violet. The mixture was stirred for 24 h and then the resulting polymer microparticles with average diameter of 4–6 μm were filtered and rinsed thoroughly with distilled water to remove the residual oxidant, water-soluble oligomer, and other by-products. The resulting black solid powders, that is, as-prepared P*p*PD salt, were left to dry in air at 50 °C for 3 days. After the P*p*PD salt had been soaked in water for 24 h, a pure P*p*PD salt was obtained. The P*p*PD base was obtained after the polymerized wet P*p*PD salts were treated with 0.2 M NH_4OH for 24 h. The poly(*o*-phenylenediamine) (P*o*PD) microparticles were also prepared in a similar way but in glacial acetic acid or water as a polymerization medium at elevated temperature.[28]

Adsorption of Pb^{2+} ions: Adsorption of Pb^{2+} ions onto poly(phenylenediamine)s was performed by using batch experiments. The effects of pH, temperature, and concentration of the Pb^{2+} solution, adsorbent dosage, and adsorption time, on the adsorption were considered. For batch tests, a given amount of poly(phenylenediamine) microparticles was added to $Pb(NO_3)_2$ aqueous solution (25 mL) at a known concentration and temperature. After a desired treatment period, the microparticles were filtered from the aqueous solution. The concentration of lead ion in the filtrate after adsorption was measured by using chemical titrimetric analysis[23,36] at a residual Pb^{2+} concentration of higher than 50 $mg\,L^{-1}$ or inductively coupled plasma (ICP) mass spectrometry at a residual Pb^{2+} concentration of lower than 50 $mg\,L^{-1}$. The adsorbed amount of lead ions on the microparticles was calculated according to Equations (7) and (8), where Q is the adsorption capacity ($mg\,g^{-1}$), q the adsorptivity (%), C_o and C the Pb^{2+} concentration before and after adsorption, ($mg\,L^{-1}$), respectively, V the initial volume of the Pb^{2+} solution (mL), and W the weight of the adsorbent added (mg).

$$Q = (C_o - C)V/W \quad (7)$$

$$q = (C_o - C)100\,\%/C_o \quad (8)$$

Characterization of structure and electrical conductivity: IR spectra were recorded on a Nicolet Nexus 470 FTIR spectrophotometer with samples prepared as KBr pellets. Wide-angle X-ray diffractograms of the microparticles were obtained with a Bruker D8 Advance X diffractometer with $Cu_{K\alpha}$ radiation at a scanning rate of 0.888° min^{-1} in a reflection mode. The size of the as-formed particles was analyzed on a Beckman Coulter LS230 laser particle-size analyzer. The bulk electrical conductivity of a pressed disk with the thickness of 20–50 μm for the microparticles was measured by a two-probe method at 20 °C.

Acknowledgements

The project was supported by the National Natural Science Foundation of China (20274030) and the Foundation of the Key Laboratory of the Molecular Engineering of Polymers (Fudan University, China). We would like to thank Prof. Yu-Liang Yang for his valuable help.

[1] P. Chen, B. Greenberg, S. Taghavi, C. Romano, D. van der Lelie, C. He, *Angew. Chem.* **2005**, *117*, 2775; *Angew. Chem. Int. Ed.* **2005**, *44*, 2715.
[2] J. Liu, Y. Lu, *J. Am. Chem. Soc.* **2003**, *125*, 6642.
[3] C. T. Chen, W. P. Huang, *J. Am. Chem. Soc.* **2002**, *124*, 6246.
[4] R. Métivier, I. Leray, B. Valeur, *Chem. Eur. J.* **2004**, *10*, 4480.
[5] J. S. Magyar, T. C. Weng, C. M. Stern, D. F. Dye, B. W. Rous, J. C. Payne, B. M. Bridgewater, A. Mijovilovich, G. Parkin, J. M. Zaleski, J. E. Penner-Hahn, H. A. Godwin, *J. Am. Chem. Soc.* **2005**, *127*, 9495.
[6] K. P. Shubha, C. Raji, T. S. Anirudhan, *Water Res.* **2001**, *35*, 300.
[7] G. N. Manju, K. A. Krishnan, V. P. Vinod, T. S. Anirudhan, *J. Hazardous Mater.* **2002**, *B91*, 221.
[8] Y. Izumi, F. Kiyotaki, T. Minato, Y. Seida, *Anal. Chem.* **2002**, *74*, 3819.
[9] B. Xiao, K. M. Thomas, *Langmuir* **2005**, *21*, 3892.
[10] S. A. Dastgheib, D. A. Rockstraw, *Carbon* **2002**, *40*, 1843.
[11] B. Hai, J. Wu, X. F. Chen, J. D. Protasiewicz, D. A. Scherson, *Langmuir* **2005**, *21*, 3104.
[12] S. M. Kraemer, J. Xu, K. N. Raymond, G. Sposito, *Environ. Sci. Technol.* **2002**, *36*, 1287.
[13] G. X. S. Zhao, J. L. Lee, P. A. Chia, *Langmuir* **2003**, *19*, 1977.
[14] R. C. Schroden, M. Al-Daous, S. Sokolov, B. J. Melde, J. C. Lytle, A. Stein, M. C. Carbajo, J. T. Fernandez, E. E. Rodriguez, *J. Mater. Chem.* **2002**, *12*, 3261.
[15] K. Z. Hossain, L. Mercier, *Adv. Mater.* **2002**, *14*, 1053.
[16] G. Y. Yan, T. Viraraghavan, *Water Res.* **2003**, *37*, 4486.
[17] P. K. Jal, S. Patel, B. K. Mishra, *Talanta* **2004**, *62*, 1005.
[18] A. Denizli, D. Tanyolac, B. Salih, E. Aydinlar, A. Qzduzal, E. Piskin, *J. Membr. Sci.* **1997**, *137*, 1.
[19] A. Denizli, D. Tanyolac, B. Salih, A. Qzdural, *J. Chromatogr. A* **1998**, *793*, 47.
[20] P. K. Roy, A. S. Rawat, P. K. Rai, *Talanta* **2003**, *59*, 239.
[21] A. Denizli, B. Salih, E. Piskin, *J. Chromatogr. A* **1997**, *773*, 169.
[22] B. Salih, A. Denizli, C. Kavakli, R. Say, E. Piskin, *Talanta* **1998**, *46*, 1205.
[23] L. M. Zhang, D. Q. Chen, *Colloids Surf. A* **2002**, *205*, 231.
[24] X. G. Li, R. Liu, M. R. Huang, *Chem. Mater.* **2005**, *17*, 5411.
[25] X. G. Li, M. R. Huang, W. Duan, Y. L. Yang, *Chem. Rev.* **2002**, *102*, 2925.
[26] X. G. Li, M. R. Huang, R. F. Chen, Y. Jin, Y. L. Yang, *J. Appl. Polym. Sci.* **2001**, *81*, 3107.
[27] X. G. Li, W. Duan, M. R. Huang, Y. L. Yang, D. Y. Zhao, Q. Z. Dong, *Polymer* **2003**, *44*, 5579.
[28] X. G. Li, M. R. Huang, Y. L. Yang, *Polymer* **2001**, *42*, 4099.
[29] T. Sulimenko, J. Stejskal, J. Prokes, *J. Colloid Interface Sci.* **2001**, *236*, 328.
[30] Y. S. Ho, G. McKay, *Process Saf. Environ. Prot.*, **1999**, *77 (B3)*, 165.
[31] Y. S. Ho, H. Benaissa, *Water Res.* **2004**, *38*, 2962.
[32] K. K. Wong, C. K. Lee, K. S. Low, M. J. Haron, *Chemosphere* **2003**, *50*, 23.
[33] B. Xiao, K. M. Thomas, *Langmuir* **2004**, *20*, 4566.
[34] C. Franco, *Eur. Polym. J.* **1996**, *32*, 43.
[35] H. S. O. Chan, S. C. Ng, T. S. A. Hor, *Eur. Polym. J.* **1991**, *27*, 1303.
[36] B. F. Senkal, N. Bicak, *React. Funct. Polym.* **2001**, *49*, 151.

Received: August 31, 2005
Revised: December 12, 2005
Published online: March 23, 2006

